Proceedings of the
Annual Stability Conference
Structural Stability Research Council
Grapevine, Texas, April 18-21, 2012

Flexural Buckling of Simply Supported Columns with "Rigid End Links" – the Key to Interpret Pin-Ended Angle Column Test Results?

E.C. Mesacasa Jr.[1], D. Camotim[2], P.B. Dinis[2], M. Malite[1]

Abstract

The paper begins by deriving and validating an analytical expression providing flexural buckling loads of uniformly compressed simply supported columns formed by a flexible central segment and two "rigid end links". It proves that the end links lower the buckling load by an amount varying with the link length, at a rate that is very high for small lengths. Then, this finding is used to re-interpret available test results on simply supported angle columns with intermediate lengths (*i.e.*, exhibiting critical flexural-torsional buckling), by showing that the rigid links used in these tests provide a mechanically sound explanation for their (apparently paradoxical) observed failure modes, involving exclusively minor-axis flexure. In order to further assess the impact of the rigid end links on the intermediate angle column structural response, the paper closes with a numerical investigation concerning the comparison between the elastic post-buckling behaviors (non-linear equilibrium paths) of columns with rigid end links exhibiting various lengths.

1. Introduction

The motivation for the work presented in this paper was provided by the quest to interpret an apparently paradoxical phenomenon that was experimentally observed in pin-ended equal-leg angle column tests. In order to explain this apparent "paradox" properly, it is convenient to begin by recalling that the critical buckling of thin-walled equal-leg angle columns occurs in either (i) local modes (very short columns), (ii) flexural-torsional modes (short-to-intermediate columns), combining major-axis flexure and torsion (since angles have no primary warping resistance, the cross-section warping constant stems exclusively from secondary warping) and (iii) minor-axis flexural modes (long columns). Fig. 1(a)-(c) provide Generalized Beam Theory (GBT) results recently reported by Dinis *et al.* (2011) concerning the buckling behavior of *fixed-ended* (F – end sections with fully restrained flexural displacements, flexural rotations, torsional rotations and warping) and *pin-ended* (P – a rather misleading designation, since the end sections only differ from the fixed ones in the fact that the minor-axis flexural rotations are free) angle columns with the same cross-section: (i) P_{cr} vs. L curves (L in logarithmic scale), (ii) modal participation diagrams and (iii) the in-plane shapes of the *5* most relevant deformation modes. It is worth noting that:

(i) The buckling behavior of the F and P short-to-intermediate columns corresponds to a "plateau" in the P_{cr} vs. L curve, which means that the critical (flexural-torsional) buckling load is almost constant within a fairly large length range. This "plateau" ends at a fairly steep descending branch, associated with critical minor-axis flexural buckling.

[1] Struct. Eng. Dept., São Carlos School of Eng., University of São Paulo,<enio.mesacasa@gmail.com; mamalite@sc.usp.br>
[2] Civil Eng. Dept., ICIST, Instituto Superior Técnico, Technical University of Lisbon, <dcamotim; dinis@civil.ist.utl.pt>

(ii) The only difference between the F and P column P_{cr} vs. L curves is the length of the above "plateau", which is obviously shortened by the release of the end section minor-axis flexural rotations – the critical buckling loads corresponding to the descending branch drop by *75%*.

(iii) Because flexural-torsional buckling is, by far, the most interesting (*i.e.*, harder to understand) instability phenomenon in equal-leg angle columns, the overwhelming majority of the investigations (analytical, numerical or experimental) focus on short-to-intermediate lengths.

(iv) The work presented in this paper deals exclusively with pin-ended columns.

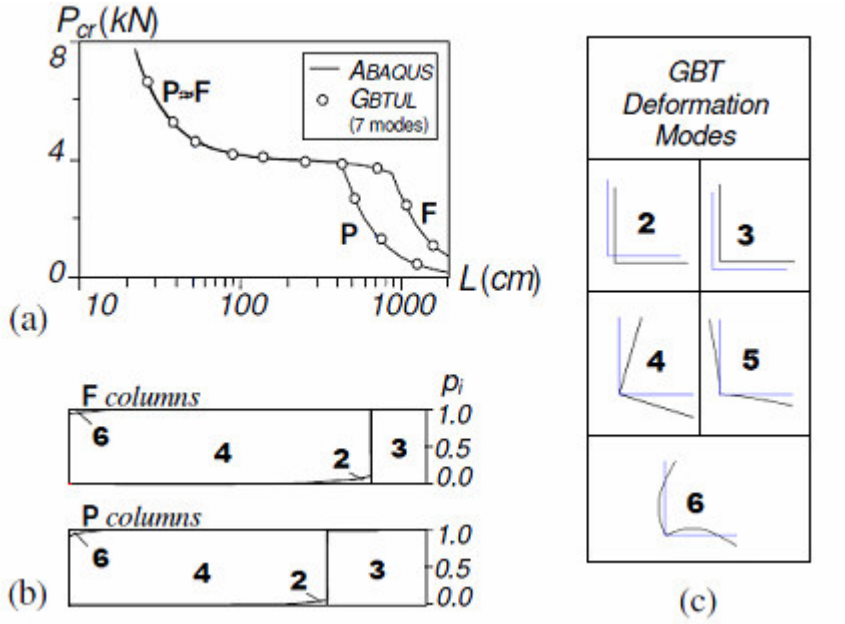

Figure 1: Buckling behavior of fixed-ended (F) and pin-ended (P) angle columns: (a) P_{cr} vs. L curves, (b) GBT modal participation diagrams, and (c) in-plane shapes of the *5* most relevant GBT deformation modes. (Dinis *et al.* 2011)

Several authors performing pin-ended angle column tests, namely Popovic *et al.* (1999), Chodraui *et al.* (2006) and Maia *et al.* (2008), reported that, surprisingly, some specimens planned and expected to provide experimental evidence of flexural-torsional buckling and collapse modes (their critical buckling loads fall well inside the P_{cr} vs. L curve "plateau") ended up failing in very clear minor-axis flexural modes. This pointed out to a relevance of minor-axis flexural buckling that was utterly unexpected, since the flexural-torsional and flexural buckling loads were supposedly quite far apart. A close inspection of

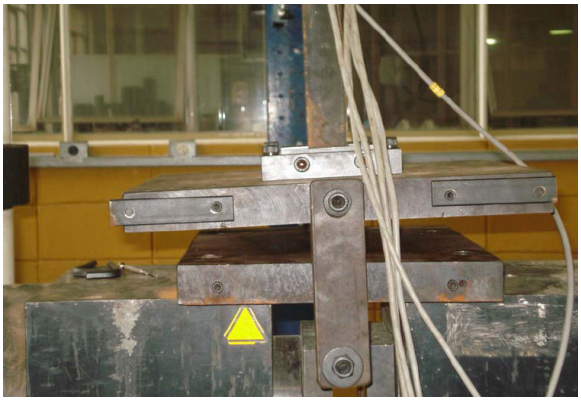

Figure 2: Typical end support arrangement in a pin-ended column test – "rigid link" and "cylindrical hinge"

the experimental set-ups adopted/described by the above researchers showed that the pin-ended column end sections were, in fact, rigidly connected to "rigid links" supported by "cylindrical hinges" at their far ends (see Fig. 2). The length of these "rigid end links" varied from case to case, but could reach a sizeable fraction of the column "real length" (excluding the links). It will be shown that the presence of these compressed "rigid end links" provides a mechanically sound explanation for the apparently paradoxical relevance of minor-axis flexural buckling. Although the column flexural-torsional buckling behavior is not affected by the "rigid end links", the same is clearly not true for minor-axis flexural buckling.

The aim of this work is to show, both analytically and numerically, that the presence of compressed "rigid end links" lowers the column flexural buckling loads, since those links behave as "leaning columns" in a sway-frame – logically (but not intuitively), the flexural buckling load drops as the link length increases. Then, this finding is shown to shed new light on the interpretation of the pin-ended angle column tests reported in the literature. Indeed, the influence of the "rigid end links" may bring the column flexural-torsional and flexural buckling loads much closer than anticipated by buckling analyses that neglect this effect – if the "rigid end links" are long enough, flexural buckling may even become critical well inside the P_{cr} vs. L curve "plateau", thus providing a logical mechanical explanation for the apparent "paradox" described earlier. In order to confirm this preliminary assessment, the pin-ended tests reported in the literature are revisited and their results are reinterpreted under the new light shed by the "rigid end link effects". Moreover, the paper also presents a brief numerical (shell finite element) study on the influence of the rigid link length on the column elastic post-buckling behavior, which shows that lower flexural buckling loads may significantly affect the pin-ended angle column strength and imperfection-sensitivity.

2. Flexural Buckling of Simply Supported Columns with Rigid End Links

As mentioned before, the presence of rigid end links affects the flexural buckling behavior of uniformly compressed simply supported (pin-ended) columns. Indeed, the (compressed) end rigid links may be viewed as "sway pin-ended columns", which means that they (i) exhibit null flexural stiffness and, thus, (ii) contribute only to the column overall geometric stiffness – *i.e.*, they have a destabilizing effect on the column flexural (in-plane) buckling behavior. Their structural role is similar to that played by a "leaning column" in a sway-frame (*e.g.*, Peng 2004), which means that the column flexural buckling load becomes progressively smaller as the end rigid link length increases.

The influence of the rigid end links on the column flexural buckling behavior can be assessed by analyzing the in-plane stability, under uniform compression, of the structural system depicted in Fig. 3(a), consisting of (i) a central column with length L_c and flexural stiffness EI, and (ii) two rigid ($EI=\infty$) end links of length L_R. This is done both (i) analytically, employing the "exact" beam finite element based on the stability functions developed by Livesley and Chandler (1956), and (ii) numerically, through standard beam finite element analyses carried out in the code ANSYS (SAS 2009). The solutions and numerical results obtained by means of these two approaches are addressed and compared next.

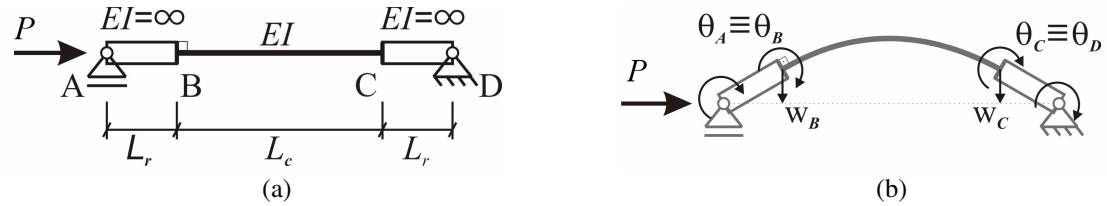

(a) (b)

Figure 3: Uniformly compressed simply supported column with rigid end links: (a) geometry and loading, and (ii) buckled configurations and degrees of freedom adopted in the "exact" finite element analysis

2.1 Analytical Solution

In order to establish the slope-deflection equations ensuring equilibrium of a column configuration adjacent to its fundamental equilibrium path ("adjacent equilibrium"), it is necessary to consider the "exact" stiffness matrices of uniformly compressed (i) fixed-ended flexible members and (ii) pin-ended rigid members – note that, in the latter case, only the (negative) stiffness associated with sway motions is involved. The fixed member stiffness matrix adopted in this work, which is based on the stability functions ϕ_i ($i=1,\ldots,4$) proposed by Livesley & Chandler (1956), is given in Fig. 4(a), together with the corresponding nodal degrees of freedom (transverse displacements and slopes at the member ends). The stability function expressions read (*e.g.*, Chen *et al.* 1996)

$$\phi_1 = \beta\,\phi_2 \cot\beta \qquad \phi_2 = \frac{\beta^2}{3(1-\beta\cot\beta)}$$
$$\phi_3 = \frac{3}{4}\phi_2 + \frac{1}{4}\beta\cot\beta \qquad \phi_4 = \frac{3}{2}\phi_2 - \frac{1}{2}\beta\cot\beta \tag{1}$$

where the dependence on the (uniform) axial force is felt through the parameter $\beta = (\pi/2)\cdot(N/N_E)^{0.5}$, relating the acting axial force N to the member Euler buckling load $N_E=\pi^2 EI/L^2$ (it coincides with the critical buckling load in simply supported members).

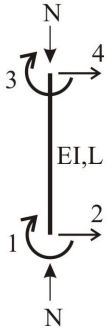

$$\left[K_{ij}^{c}\right] = \frac{EI}{L}\begin{bmatrix} 4\phi_3 & \frac{6\phi_2}{L} & 2\phi_4 & \frac{-6\phi_2}{L} \\ \frac{6\phi_2}{L} & \frac{12\phi_1}{L^2} & \frac{6\phi_2}{L} & \frac{-12\phi_1}{L^2} \\ 2\phi_4 & \frac{6\phi_2}{L} & 4\phi_3 & \frac{-6\phi_2}{L} \\ \frac{-6\phi_2}{L} & \frac{-12\phi_1}{L^2} & \frac{-6\phi_2}{L} & \frac{12\phi_1}{L^2} \end{bmatrix}$$

(a)

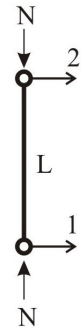

$$\left[K_{ij}^{r}\right] = \frac{N}{L}\begin{bmatrix} -1 & 1 \\ 1 & -1 \end{bmatrix}$$

(b)

Figure 4: "Exact" stiffness matrices concerning uniformly compressed (a) fixed and (b) rigid pinned members.

As for the pin-ended rigid member stiffness matrix, which stems from linear displacement functions, it is displayed in Fig. 4(b), with the corresponding end transverse displacements associated with rigid-body motions (Gonçalves 2000). Note the null stiffness matrix determinant, meaning that this member cannot sustain equilibrium by itself – indeed, it must "lean on" the remaining structural system to acquire the additional stiffness required to compensate for its "inherent instability".

Taking into account that the column degrees of freedom are constrained to satisfy the conditions $w_B=L_r\,\theta_A$ and $w_C=-L_r\,\theta_D$ (see Fig. 3(b)), adjacent equilibrium only occurs if the equation system

$$\begin{bmatrix} M_A \\ M_D \end{bmatrix} = \begin{bmatrix} L_r^{\,2}(-A+B) + 2L_rC + D & L_r^{\,2}B + 2L_rC + E \\ L_r^{\,2}B + 2L_rC + E & L_r^{\,2}(-A+B) + 2L_rC + D \end{bmatrix} \cdot \begin{bmatrix} \theta_A \\ \theta_D \end{bmatrix} = 0 \tag{2}$$

is satisfied, where

$$A = \frac{N}{L_r} \qquad B = \frac{12\phi_1 EI}{L_c^{\,3}} \qquad C = \frac{6\phi_2 EI}{L_c^{\,2}}$$
$$D = \frac{4\phi_3 EI}{L_c} \qquad E = \frac{2\phi_4 EI}{L_c} \tag{3}$$

and the two equations stand for the moment equilibrium of rigid links AB and CD. The column buckling (bifurcation) loads are the non trivial solutions of the eigenvalue problem defined by (2), *i.e.*, the roots of the associated characteristic equation

$$\left(AL_r^{\,2} - D + E\right)\left(AL_r^{\,2} - 2BL_r^{\,2} - 4CL_r - D - E\right) = 0 \tag{4}$$

the lowest of which is the "critical buckling (bifurcation) load". The next section presents and discusses illustrative examples concerning the influence of the rigid end links on the minor-axis flexural buckling behaviour of uniformly compressed pin-ended equal-leg angle columns. The solutions provided by (4) are also compared with values yielded by ANSYS beam finite element analyses.

2.2 Illustrative Examples and ANSYS Numerical Results

The numerical results concern columns with $E=20000\,kN/cm^2$, $I=1\,cm^4$, $L_c=100\,cm$ and L_r comprised between *0* and $300\,cm$, which corresponds to $0 \le L_r/L_c \le 3.0$ – obviously, $L_r=0$ corresponds to Euler's column and $P_{cr} \equiv P_E = 19.739\,kN$. Moreover, the validation of the analytical solution derived in the previous section is made trough the comparison with some values yielded by standard beam finite element analyses carried out in the code ANSYS[3].

The curves plotted in Figs. 5 and 6 provide the variation of the column critical buckling load P_{cr}, normalized with respect to P_E, with the link-to-column length ratio L_r/L_c, for two situations: (i) L_c remains unchanged as L_r increases, corresponding to a column with total length $L_{tot}=2\times L_r+L_c$ (Fig. 5), and (ii) L_c decreases as L_r increases, so that the column total length remains unaltered (Fig. 6). The observation of these buckling results prompts the following comments and remarks:

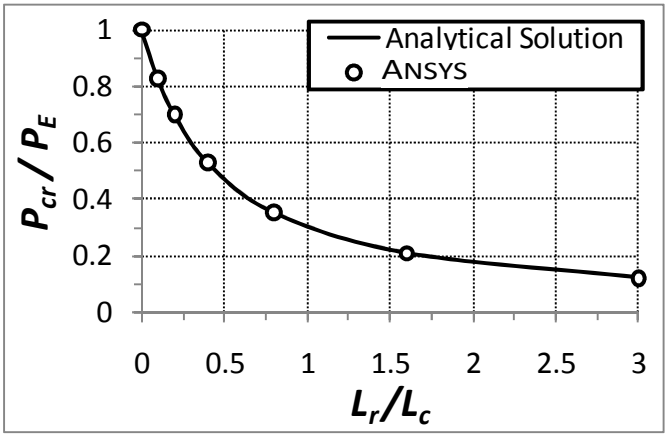

Figure 5: Illustrative example: variation of P_{cr}/P_E with L_r/L_c (for L_c constant)

[3] Both the flexible column and the rigid end links were modeled by means of BEAM3 finite elements (*2* nodes and *3* degrees of freedom per node). The discretization adopted involved (i) *6* elements in the column and (ii) *1* element per rigid end link – the rigidity of the latter was ensured by considering a large bending stiffness value ($EI=1\times10^8\,kNcm^2$). The rigid links were provided with pinned end supports (free rotation and null transverse displacement), one of which was free to move axially.

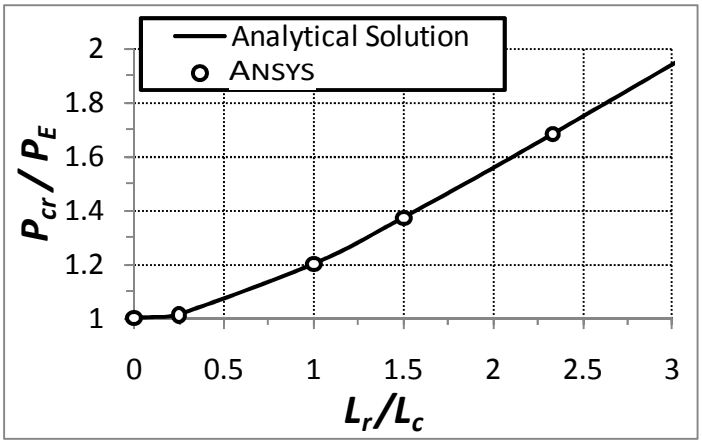

Figure 6: Illustrative example: variation of P_{cr}/P_E with L_r/L_c (for $L_{tot}=2\times L_r+L_c$ constant)

(i) First of all, there is a perfect coincidence between the analytical and ANSYS P_{cr} values, thus confirming the correctness of equations (2) and (4).

(ii) When L_c is kept constant, which implies that two "leaning" rigid end links are added to Euler's column, P_{cr} decreases monotonically as L_r increases. Moreover, it is worth noting that the decreasing rate is particularly high for small L_r values and becomes progressively lower as L_r grows. For instance, when L_r increases from *0* to *5 cm* ($L_r/L_c=0.05$), P_{cr} drops from *19.739* to *16.333 kN*, *i.e.*, about *17%*. On the other hand, a L_r increase from *15* to *20 cm* causes a P_{cr} drop of no more than *8%*.

(iii) The high initial decreasing rate is due to the combination of two concurrent destabilizing factors: (iii_1) the total length increase and (iii_2) the added negative stiffness brought about by the rigid links, which also depends on the length, since, in percentage terms, the length increase becomes gradually less important as L_r/L_c grows, the decreasing rate becomes progressively smaller.

(iv) When the total length L_{tot} is kept unchanged, thus meaning that the flexible Euler's column end segments are replaced by rigid links, P_{cr} increases monotonically with L_r. However, in this case the growing rate is virtually imperceptible for small L_r values (up until $L_r/L_c\approx0.25$) and then, after a fairly fast transition, becomes practically constant (*i.e.*, P_{cr}/P_E becomes proportional to L_r/L_c).

(v) The minute initial growing rate is due to the fact that the flexible column segments first replaced by rigid links are those exhibiting smaller bending curvatures (*i.e.*, the replacement is barely beneficial). As L_r/L_c increases, the replacement involves gradually "more curves" column segments and, therefore, the above growing rate becomes progressively larger.

2.3 Implications on the buckling behavior of intermediate pin-ended angle columns

It has been shown that the buckling behavior of the so-called pin-ended[4] equal-leg angle columns with intermediate lengths is characterized by (i) critical buckling loads associated with (major-axis) flexural-torsional modes and (ii) non-critical buckling loads corresponding to (minor-axis) flexural modes. Moreover, these buckling load pairs become progressively closer as the column length increases, until a "switch" occurs and the minor-axis flexural buckling loads become the critical ones – see Fig. 1(a).

In pin-ended angle column tests, the presence of the rigid end links means that the lengths involved in (major-axis) flexural-torsional modes and (minor-axis) flexural buckling are not the same. Indeed, while (i) flexural-torsional buckling is governed by the flexible column length L_c (recall that the end

[4] End supports that (i) fully restrain major/minor-axis flexural displacements, major-axis flexural rotations, torsional rotations and (secondary) warping, while (ii) freely allowing minor-axis flexural rotations.

supports prevents major-axis flexural rotations), (ii) the total length (including the rigid end links) comes into play in flexural buckling. This buckling length discrepancy brings the two buckling loads closer than antecipated by a buckling analysis based solely on L_c, by an amount depending on the rigid link length L_r (if L_r is "large enough", the flexural buckling load may even fall below its flexural-torsional counterpart). Neglecting this rigid end link effect may lead to surprising (or even "paradoxical") findings and/or erroneous result interpretations in experimental tests involving pin-ended equal-leg angle columns with intermediate lengths – this issue will be addressed further ahead in the paper.

3. Interpretation of the Available Tests on Pin-Ended Angle Columns

The initial purpose of this section is to identify and gather available test data concerning pin-ended equal-leg angle columns with intermediate lengths, in the sense that their (theoretical) critical buckling loads correspond to flexural-torsional buckling, *i.e.*, fall on the P_{cr} *vs.* L curve plateau shown in Fig. 1(a). It was found that tests fulfilling these requirements were carried out by Popovic *et al.* (1999), Chodraui *et al.* (2006) and Maia *et al.* (2008) – the geometrical and material properties of all the tested column specimens identified are given in Table 1. For each of them, Table 2 provides the reported (i) column length (L_c), (ii) rigid end link length (L_r), (iii) experimental ultimate load ($P_{u.exp}$) and (iv) observed failure mode: either major-axis flexural-torsional (FT), minor-axis flexural (F) or a combination of both (F+FT) – one (F+FT) failure was associated with the occurrence of a "snap through" (ST) phenomenon. Moreover, in order to provide a better visualisation of the buckling characteristics of each column specimen identified, Figs. 7-11 provide the locations of their lengths on the corresponding three buckling curves (P_b *vs.* L), associated with (i) flexural-torsional buckling (which includes the P_{cr} *vs.* L plateau), (ii) minor-axis flexural buckling based on the flexible column length L_c, *i.e.*, neglecting the rigid end links, and (iii) minor-axis flexural buckling based on the total length L_{tot}, *i.e.*, accounting for the rigid links – recall that the rigid end links do not influence flexural-torsional buckling.

The joint observation of the values reported in Table 2 and the results displayed in Figs. 7-11 leads to the following conclusions:

(i) In each test series there exists at least one column specimen for which the consideration of the rigid end links lowers the minor-axis flexural buckling load below its flexural-torsional counterpart. Moreover, the presence of the rigid end links brings the two buckling loads very close together for several other column specimens.

(ii) All but one of the column specimens with minor-axis flexural buckling loads lower or very close to their flexural-torsional counterparts, the experimentally observed failure modes exhibited evidence of minor-axis flexure, either alone (F) or combined with major-axis flexure and torsion (F+FT). The exception is the column specimen tested by Maia *et al.* (2008) with L_c=*145 cm*, combining an observed flexural-torsional (FT) failure mode with a critical minor-axis flexural buckling.

(iii) The role played by the rigid end links is clearly more relevant in the column specimens tested by Popovic *et al*. (1999), depicted in Figs. 7-9, than in those reported by Chodraui *et al.* (2006) and Maia *et al*. (2008), displayed in Figs. 10-11. This is due to the fact that the corresponding L_r/L_c values are much higher – indeed, these values range between (iii$_1$) *0.35* and *0.11* (Popovic *et al*. 1999), (iii$_2$) *0.14* and *0.04* (Chodraui *et al.* 2006) and (iii$_3$) *0.14* and *0.05* (Maia *et al.* 2008).

(iv) Only one column specimen combines a failure mode exhibiting only minor-axis flexure with a lower flexural-torsional buckling load: the one tested by Maia *et al.* (2008) with L_c=*100 cm*.

(v) There are several column specimens, exhibiting both minor-axis flexural and flexural-torsional critical buckling, whose observed failure modes involve minor-axis flexure, major-axis flexure and torsion (F+FT). Most likely, the explanation for this fact lies in the configurations of the column

Table 1: Geometrical and material properties of all the specimens tested and identified pin-ended columns

	Specimen	b_f (*cm*)	*t* (*cm*)	I_{min} (cm^4)	*A* (cm^2)	$r_{mín}$ (*cm*)	f_y (*MPa*)	*E* (*MPa*)
***Popovic et al.* (1999)**	L50x2.50	5.00	0.231	2.1866	2.260	0.984	396	207100
	L50x4.00	5.037	0.379	3.3704	3.607	0.967	388	209800
	L50x5.00	5.047	0.470	4.0172	4.420	0.953	388	207400
***Chodraui et al.* (2006)**	L60x2.25	6.00	0.238	3.9100	2.773	1.188	371	205000
***Maia et al.* (2008)**	L60x2.25	6.00	0.238	3.9100	2.773	1.188	357	205000

Table 2: Reported tested specimen lengths (column and rigid links), ultimate loads and observed failure modes

	Specimen	***Test***	L_c (*cm*)	L_r (*cm*)	$P_{u.exp}$ (*kN*)	***Failure****
Popovic *et al.* (1999)	**L 50x2.5**	***1***	28.6	10.0	41.7	FT
		2	28.5	10.0	47.2	FT
		3	49.0	10.0	35.2	F+FT
		4	49.0	10.0	40.1	F+FT (ST)
		5	67.4	10.0	30.9	F+FT
		6	67.5	10.0	47.5	F
		7	90.0	10.0	25.1	F+FT
		8	90.0	10.0	32.1	F
	L50x4.0	***1***	28.5	10.0	13.7	F+FT
		2	49.0	10.0	105.0	F
	L 50x5.0	***1***	28.5	10.0	154.8	F
		2	49.0	10.0	119.1	F+FT
		3	49.0	10.0	117.3	F
Chodraui *et al.* (2006)	**L 60x2.38**	***1***	48.0	6.75	31.0	F+FT
		2	83.5	6.75	29.0	F+FT
		3	119.5	6.75	23.0	F+FT
		4	155.0	6.75	21.0	F+FT
Maia *et al.* (2009)	**L 60x2.38**	***1***	48.0	6.75	31.0	FT
		2	65.0	6.75	36.1	FT
		3	83.5	6.75	29.0	FT
		4	100.0	6.75	39.8	F
		5	119.5	6.75	22.5	FT
		6	135.0	6.75	28.5	F
		7	145.0	6.75	21.0	FT

*Failure modes: F – minor-axis flexural; FT – flexural-torsional; ST – "snap-through"

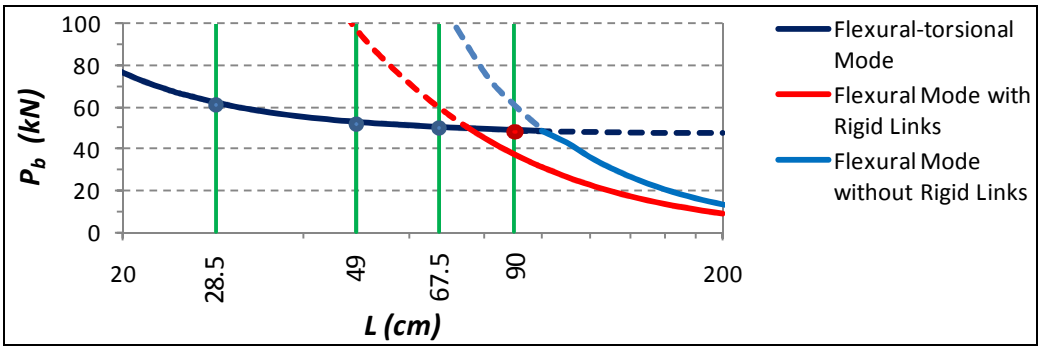

Figure 7: P_b *vs L* curves and lengths of the column specimens tested by Popovic *et al.* (1999) – L50x2.50

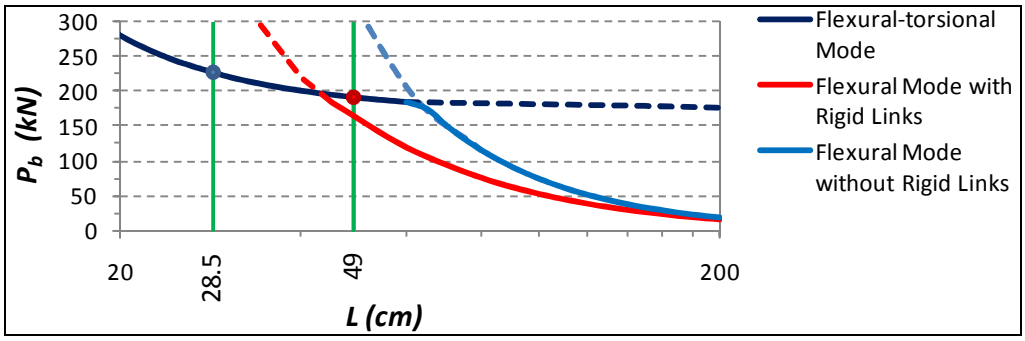

Figure 8: P_b *vs* L curves and lengths of the column specimens tested by Popovic *et al.* (1999) – L50x4.00

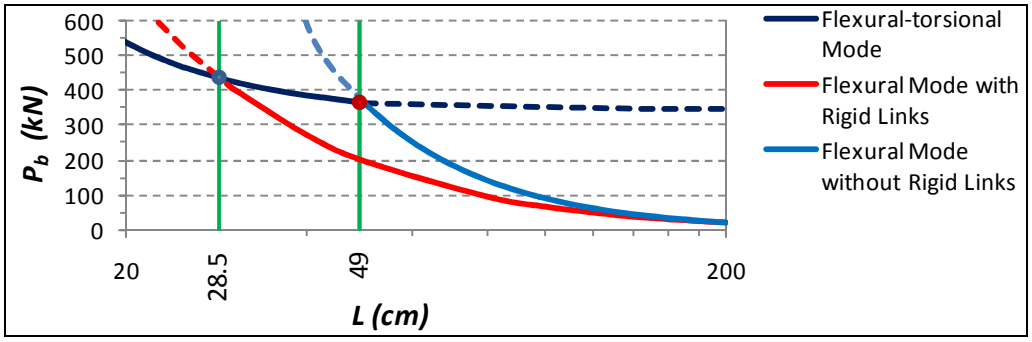

Figure 9: P_b *vs* L curves and lengths of the column specimens tested by Popovic *et al.* (1999) – L50x5.00

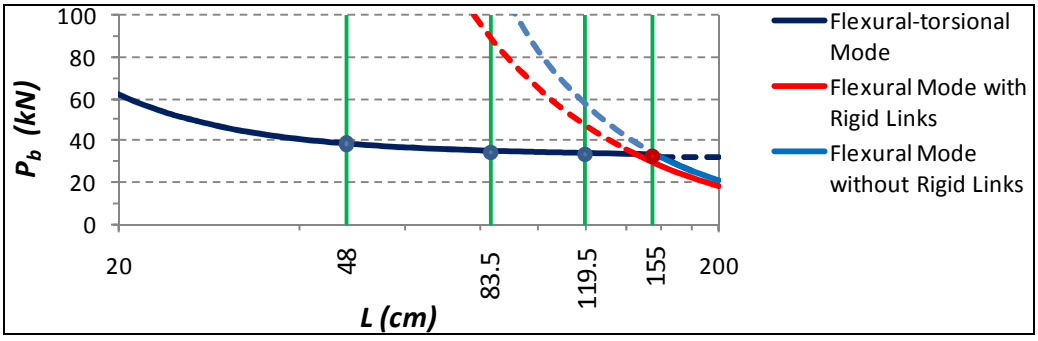

Figure 10: P_{cr} *vs* L curve and lengths of the column specimens tested by Chodraui *et al.* (2006) – L60x2.38

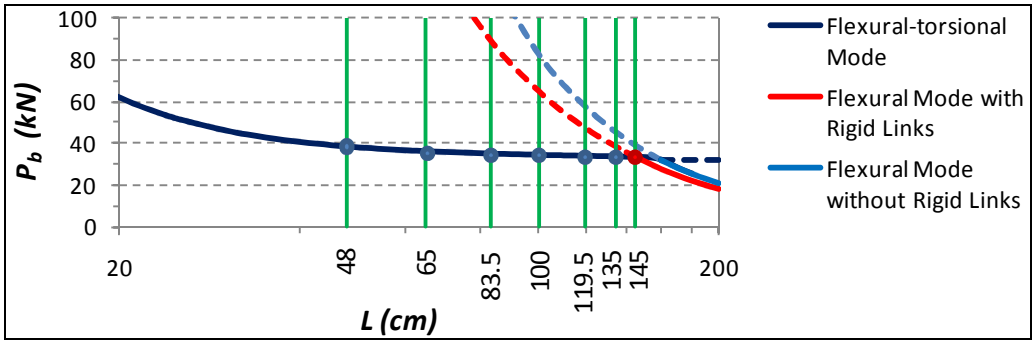

Figure 11: P_b *vs* L curves and lengths of the column specimens tested by Maia *et al.* (2008) – L60x2.38

initial geometrical imperfections, which may be more akin to the non-critical buckling mode shape. This issue is further addressed in the next section, where the influence of the rigid end links on the column elastic post-buckling behavior is investigated.

4. Influence of the Rigid End Links on the Column Elastic Post-Buckling Behavior

In order to assess the influence of the rigid end links on the elastic post-buckling behavior of pin-ended angle columns, geometrically non-linear analyses of two columns tested by Popovic *et al*. (1999), namely those with a *L50x2.50* cross-section and lengths L_c=*67.5 cm* and L_c=*90 cm* (values corresponding to distinct location in the P_{cr} *vs* L_c curve plateau – see Fig. 7). The columns analyzed exhibit rigid end links with four different lengths, varying between *0* and *30 cm*, and all of them contain flexural-torsional initial geometrical imperfections with an amplitude (maximum mid-height transverse displacement) equal to *10%* of the wall thickness[5]. The analyses were carried out in the code ANSYS (SAS 2009) (i) discretizing the columns into fine meshes of 4-node isoparametric shell finite elements (SHELL181) and (ii) modelling the rigid end links by means of exactly the same shell elements, which are assumed to exhibit a very large Young's modulus ($2x10^{14}$ *kN/cm*^{2}). In order to simulate the column intermediate boundary conditions, the flexible column end sections are fixed to the rigid end links, thus ensuring full warping and local displacement/rotation restraints. The rigid link end supports are materialized by means of rigid plates that are only allowed to (i) move longitudinally and (ii) rotate about the column minor-axis.

Figs. 12(a)-(b) (L_c=*67.5 cm*) and 13(a)-(b) (L_c=*90 cm*) depict the column P/P_{cr} *vs.* α and P/P_{cr} *vs.* d_m equilibrium paths, where (i) α and d_m stand for the mid-height torsional rotation and displacement along the major-axis (due to minor-axis flexure) and (ii) the applied load is normalized with respect to the critical load of the columns without rigid end links (*i.e.*, P_{cr} corresponds to flexural-torsional buckling). Five rigid end link lengths are considered, namely L_r=*0; 5; 10; 20; 30 cm* – recall that L_r=*10 cm* was the length measured and reported by Popovic *et al*. (1999). The observation of these fours sets of elastic non-linear equilibrium paths prompts the following remarks:

(i) First of all, it is important to mention that all columns exhibit a clearly dominant deformation pattern, which may be either (i_1) flexural-torsional (large α values and much smaller d_m values) or (i_2) minor-

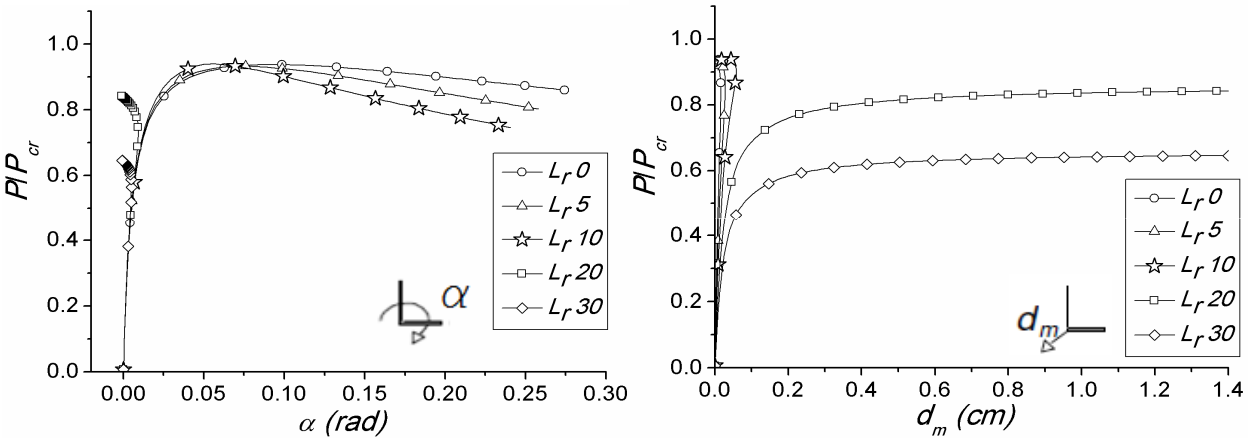

Figure 12: (a) P/P_{cr} *vs* α and (b) P/P_{cr} *vs* d_m equilibrium paths of the *50x2.25 mm* with L_c=*67.5 cm* (five L_r values).

[5] No minor-axis flexural initial geometrical imperfections are considered in this work. Nevertheless, the authors are fully aware of the relevance of such initial geometrical imperfections, which are bound to have a strong influence on the column post-buckling behavior (elastic or elastic-plastic) and ultimate strength. Moreover, given the cross-section minor-axis asymmetry, the sign/direction of the initial out-of-straightness (causing compressions along either the corner or the free longitudinal edges) is also expected to play a very important role in the column imperfection-sensitivity with respect to initial minor-axis flexure. It is worth mentioning that the authors are currently investigating the joint influence of the rigid end links and initial geometrical imperfection shape on the post-buckling behavior and ultimate strength of pin-ended equal-leg angle columns – the outcome of this investigation will be reported in the near future.

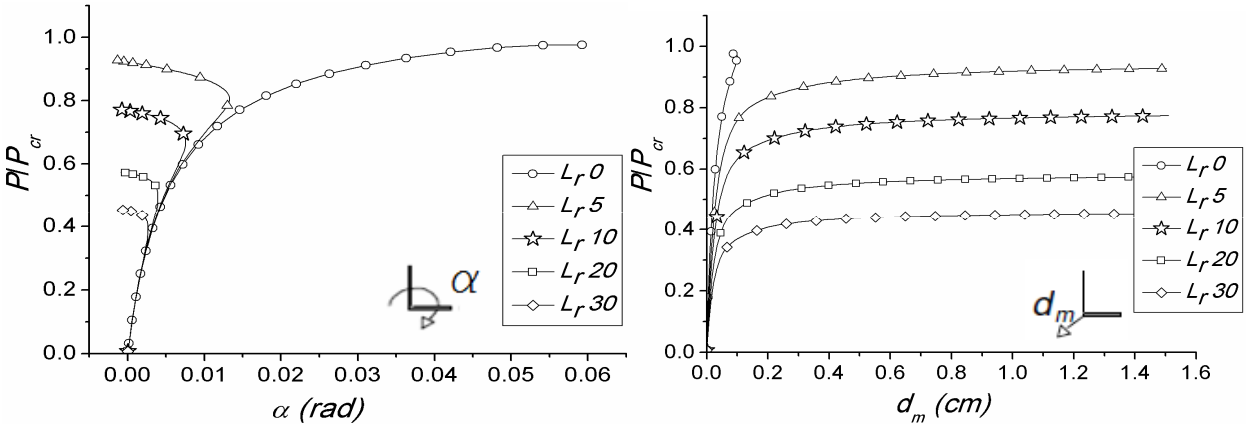

Figure 13: (a) P/P_{cr} *vs* α and (b) P/P_{cr} *vs* d_m equilibrium paths of the *50x2.25 mm* with L_c=*90.0 cm* (five L_r values).

axis flexural (large d_m values and much smaller α values) – in the latter case, there is a dramatic deformation pattern switch, since only flexural-torsional initial geometrical imperfections were included in the shell finite element analyses.

(ii) In the L_c=*67.5 cm* columns, the flexural-torsional and minor-axis flexural deformation patterns are dominant for L_r=*0*;*5*;*10 cm* and L_r=*20; 30 cm*, respectively. As it would be logical to expect, these L_r value sets correspond to critical flexural-torsional and minor-axis flexural buckling, respectively.

(iii) The L_c=*67.5 cm* columns with rigid end link lengths up to L_r=*10 cm* exhibit quite well defined (elastic) limit points, occurring for small-to-moderate torsional rotations, and very similar ultimate loads. This means that failure is exclusively due to geometrically non-linear effects and also that the ultimate load is fairly insensitive to the rigid end link length L_r.

(iv) The L_c=*67.5 cm* columns with rigid end link lengths higher than L_r=*10 cm* exhibit no limit point and quite different ultimate loads, as defined by the corresponding plateaus. This means that plasticity is required to trigger the column failure and also that the ultimate load decreases visibly with L_r.

(v) In the L_c=*90 cm* columns, the flexural-torsional deformation pattern is only (marginally) dominant in the absence of rigid end links (L_r=*0*) – the only case for which flexural-torsional buckling is critical. In the presence of rigid links, the minor-axis flexural deformation pattern becomes dominant and, as before, there is considerable strength erosion as L_r increases – this can be assessed by looking at the vertical distance between the various P/P_{cr} *vs.* d_m equilibrium paths (they are quite far apart).

(vi) The joint observation of the equilibrium paths concerning L_r=*10 cm*, Fig. 7 and Table 2 reveals that there is fairly good agreement between these numerical results and the failure modes observed in the tested column specimens. Indeed, for both L_c=*67.5 cm* and L_c=*90 cm* there were two column specimens tested and, in each case, one specimen failed in a pure minor-axis flexural (F) mode and the other in a combination of minor-axis flexure, major-axis flexure and torsion (F+FT). This is in line with the fact that the corresponding critical and non-critical buckling loads (accounting for the rigid end link effect) are quite close together – it makes it perfectly logical that either one or both of these two "ingredients appear in the failure mode (recall that it is an elastic-plastic collapse, while the equilibrium paths displayed are purely elastic). However, it is worth noting that a mechanically sound explanation for the fact that practically identical columns fail in different modes is still lacking. The authors believe that the root of such an explanation lies in the combined effect of the rigid end links and the initial geometrical imperfection shape – as mentioned before, the implications of this combined effect on the column ultimate strength and failure mode are currently under investigation.

5. Concluding Remarks

This paper began by demonstrating, both analytically and numerically, that the addition of rigid end links to a uniformly compressed simply supported column lowers its flexural buckling loads, since those links behave as "leaning columns" in a sway-frame – indeed, it was shown that the flexural buckling load drops as the link length increases. Then, this somewhat surprising finding was used to shed new light on the interpretation of the pin-ended equal-led angle column tests reported in the literature. It was shown that the presence of the rigid end links with lengths typically employed in experimental set-ups may bring the column flexural-torsional and minor-axis flexural buckling loads much closer than anticipated by buckling analyses that neglect this presence – in fact, for long enough links flexural buckling becomes critical well inside the P_{cr} vs. L curve "plateau" commonly associated with critical flexural-torsional buckling, thus providing a mechanically sound explanation for some apparently "paradoxical" behaviors that were reportedly observed in experimental tests. In order to confirm this preliminary assertion, the pin-ended angle column tests reported in the literature were revisited and their results were reinterpreted under the new light shed by the "rigid end link effects". Moreover, the paper also presents a limited shell finite element study aimed at assessing how the rigid link length affects the column elastic post-buckling behavior, which showed that the lower flexural buckling loads significantly influence the pin-ended angle column strength and imperfection-sensitivity.

Finally, just two words to mention that the authors are currently investigating the joint influence of the rigid end links and initial geometrical imperfection shape on the non-linear behavior and ultimate strength of pin-ended angle columns. The results obtained, which should have far-reaching implications on the development of an efficient design procedure for these elusive structural members, will be reported soon.

Acknowledgments

The first and fourth authors acknowledge the financial support of the National Council for Scientific and Technological Development (CNPq - Brazil) and the Foundation of Research Increase and Industrial Improvement (FIPAI - Brazil). The second and third authors acknowledge the financial support provided by *Fundação para a Ciência e Tecnologia* (FCT – Portugal), through the research project "Generalised Beam Theory (GBT) – Development, Application and Dissemination" (PTDC/ECM/108146/2008).

References

Chen WF, Goto Y, Liew JYR (1996). *Stability Design of Semi-Rigid Frames*, John Wiley & Sons, New York.

Dinis PB, Camotim D, Silvestre N (2011). On the mechanics of thin-walled angle column instability, *Thin-Walled Sructures*, **52**, 80-89, March 2012.

Chodraui GMB, Shifferaw Y, Malite M, Schafer BW (2006). Cold-formed steel angles under axial compression, *Proceedings of 18th International Specialty Conference on Cold-Formed Steel Structures* (St. Louis, 26-27/10), R. LaBoube, W.-W. Yu (eds.), 285-300.

Gonçalves R (2000). *Local Imperfections in Steel Structures: Concepts, Results and Thoughts*, M.A,Sc. Thesis in Structural Engineering, Instituto Superior Técnico, Technical University of Lisbon. (Portuguese)

Livesley RK, Chandler DB (1956). *Stability Functions for Structural Frameworks*, Manchester University Press.

Maia W F, Neto JM, Malite M (2008). Stability of cold-formed steel simple and lipped angles under compression, *Proceedings of 19th International Specialty Conference on Recent Research and Developments in Cold-Formed Steel Design and Construction* (St. Louis, 14-15/10), R. LaBoube, W.-W. Yu (eds.), 111-125.

Popovic D, Hancock GJ, Rasmussen KJR (1999). Axial compression tests of cold-formed angles, *Journal of Structural Engineering* (ASCE) **125**(5), 515-523.

Peng JL (2004). Structural modeling and design considerations for double-Layer shoring systems. *Journal of Construction Engineering and Management*, **130**(3), 368-377.

SAS (Swanson Analysis Systems Inc.) (2009). *ANSYS Reference Manual* (version 12).